Studies on the influence of corrosion and wear resistant SnS coatings on Aluminum 6061 alloy

K. Shanmugapriya, D. Rajagopal and S. Karthikeyan*

Department of chemistry, SAS, Vellore Institute of Technology, Vellore, 632 014, India

**E-mail: skarthikeyanphd@yahoo.co.in*

Abstract

The impact of electroless Ni-P-SnS coatings on Al 6061 alloy was studied in this work. Tin (II) sulfide was added to the Ni-P matrix using the electroless deposition technique. The tin sulfide particles added increased the Ni-P coatings on Al 6061's hardness and corrosion resistance. Intermetallic phases formed in the coatings in a manner that was shown by XRD measurements. Both the hard tin sulfide particles and the Ni_3P phases present in the coatings matrix attributed for the harder material value of coatings comprising Ni – 8.87% P – 7.62% SnS. Wear resistance of Ni – 8.87% P – 7.62% SnS is higher than that of Ni – 10.84% P – 0% SnS, indicating that SnS particles in the coatings are the reason for the better outcomes. The incorporation of SnS particles in the Ni-P matrix was found to increase the roughness of coated surfaces. Al 6061 alloy with annealed SnS incorporation and electroless Ni-P coatings has superior corrosion resistance than Al 6061 alloy with 3.5% NaCl, as is well demonstrated. The electroless Ni-P-SnS coatings produced on Al 6061 were shown to have lower coefficients of friction than Ni-P coatings under difficult sliding conditions. The wear resistances of the coatings have improved after the heat treatment procedure. The Ni-P-SnS coatings are said to be capable of serving as solid lubricants for the sliding components of machinery employed in the electronic sectors.

Received: May 10, 2023. Published: June 23, 2023 doi: 10.17675/2305-6894-2023-12-2-22

Keywords: *wear, composites, lubricants, coatings, corrosion.*

1. Introduction

The flexible aluminum metal and its alloys are extensively used in the automotive, electronic, and other industries. However, because of their weak resistance to wear and corrosion, aluminum and its alloys' surfaces need protection. By suspending ceramic powders in the plating solution as a suspension during the plating process, electroless composite coatings such as Ni-P-Al_2O_3 [1], Ni-P-MoS_2 [2, 3], Ni-P-PTFE [4–6], Ni-P-SiC [7–9], Ni-P-graphite [10], and a few other coatings [11–13] were carried out. This allowed the powders to be incorporated into the coating matrix. Because of the following factors, aluminum alloys are "difficult to plate metal": (i) the presence of a passive oxide layer on their surface, which reduces the coatings' adherence; (ii) the inhomogeneous microstructure consisting of the primary phase and the second phase will result in the uneven coatings; As a result, electroless plating on aluminum alloys faces a serious obstacle. Composite coatings embedded with transition metal dichalcogenides (disulfides), such as MoS_2, SnS, *etc*., with low friction need to be developed in order to meet the demands for sliding parts with low friction, good wear and corrosion resistance under dry conditions, particularly for aerospace industries. Tin (II) sulfide is one of them and yet has good lubricating and corrosion resistance properties. Due to SnS's hydrophobic characteristics, its inclusion into the electroless plating process causes complications. This work produced a method for the electroless composite plating of Ni-P-SnS on Al alloy. Then, it was determined how the multilayer coatings, which included electroless Ni-P-SnS and Ni-P coatings, performed mechanically.

2. Materials and Methods

Al 6061 aluminum samples with dimensions of $10\ cm\times10\ cm\times3\ mm^3$ were used as the substrates. Specimens were mechanically polished with SiC paper to a grit of 1000 before being ultrasonically degreased in trichloroacetone. Alkaline cleaning, double zincating, activating, electroless Ni-P plating, and Ni-P-SnS composite plating were all steps involved in this plating process. The following were the electroless plating Ni-P compositions and conditions: nickel carbonate $22\ g\cdot l^{-1}$, sodium hypophosphite $34\ g\cdot l^{-1}$, tri sodium citrate $40\ g\cdot l^{-1}$, ammonium fluoride $9\ g\cdot l^{-1}$, lead nitrate $0.02\ g\cdot l^{-1}$, pH 5.5, temperature 90°C. To the above electroless plating solution, $2–20\ g\cdot l^{-1}$ of SnS (size – 2 μm) were introduced to the electroless plating solution. Before addition, the tin sulfide particles were blended with small amount of SLES wetting agent ($0.1\ g\cdot l^{-1}$) and made as sludge. The bath was agitated by mechanical stirrer with 420 rpm. The deposit thickness was 40 microns measured using XRF spectroscopy (AMI, USA).

By completely precipitating phosphorus as ammonium phosphomolybdate, dissolving the precipitate in 1 N HNO_3, and estimating the excess HNO_3 by back titration, the amount of phosphorus in the Ni-P deposits was determined. By complexometric titration with EDTA and murexide as the indicator, nickel was examined. The formula C=(weight of SnS / coating weight)×100 was used to determine the amount of SnS in composite coatings. Deposits of Ni and P were fully dissolved in the HNO_3 solution. However, SnS particles were insoluble in HNO_3. To ensure the total precipitation of SnS particles, the entire solution was held for a week. The SnS particles were then separated and dried for 12 hours at 95°C. The dried SnS particles were then accurately weighed to 0.01 mg on an electronic scale.

Using an Innova SPM Atomic Force Microscope (AFM), all of the sample surfaces' surface morphology and surface roughness were examined. An AFM's tip was moved continuously across an electroless nickel-plated surface to produce a three-dimensional image of the surface's features. Piezoelectric motors are used to move the tip over the surface, and the force between the tip and the surface is maintained by monitoring the position of the tip using light reflected from it.

Vickers hardness coated composites were tested at a load of 100 g and annealed at 250°C using a diamond pyramid indenter technique with a 15-second indentation period.

The results were measured five times on average. With a properly calculated constant force applied to the test specimen, a 4-sided square-based pyramid indenter was used in the Vickers hardness test to measure the indentation's surface area. The specimen was initially raised till it touches the indenter. The indenter then applies the test force on the test specimen, gradually raising it until it achieves the desired value. Following the required dwell time, this force was maintained, and the surface area of the diamond- or square-shaped depression was computed. After that, the following formula was used to determine the material's Vickers hardness:

Vickers Hardness, *HV*, is calculated as follows:

$$HV = 1.854 \times (F / D^2)$$

or applied test force in kilogram-forces (kgf) per surface area of indentation (mm^2).

Taber abrasion resistance with CS-10 abrasive wheel having a load of 1 kg for 1000 cycles was done on Ni-P and Ni-P-SnS coatings.

EG and G Princeton Applied Research Model 6310 was employed for corrosion resistance studies. To that extent, one cm^2 electrolessly deposited Ni-P and Ni-P-SnS were prepared and used as working electrodes. 4 cm^2 of platinum and saturated calomel electrodes were adapted as auxiliary and reference electrodes. The electrolyte was 3.5% NaCl.

Frictional coefficient studies were conducted using a pin-on-disc tribometer as per ASTM G99-05. Samples were mounted on a stationary holder after being cut into 10 mm×10 mm squares. With a force of 3 N, the specimen was placed onto a disc, which then had 220 grit SiC abrasive paper adhered to it. For 10 minutes, the disc was rotated at a constant speed of 5 rpm while the samples slid at a rate of 15.7 mm per second.

3. Results and Discussion

3.1. Surface Roughness measurements

Table 1 reviews the surface roughness values of Ni-P-SnS and polished Al 6061 surfaces. It was observed that the incorporation of SnS particles in Ni-P matrix had increased roughness of coatings surfaces.

Table 1. AFM data for composite coatings.

Samples	Root mean square roughness, R_q	Average roughness, R_a	Mean of maximum Peak-to-Valley Height
Polished Al 6061 alloy	0.021 (μm)	0.016 (μm)	0.074 (μm)
EN-P coatings on Al 6061 alloy	132.20 (nm)	119.12 (nm)	421.6 (nm)
EN-P-SnS coatings on Al 6061 alloy	45.88 (nm)	40.23 (nm)	156.41 (nm)

Table 2. Hardness and wear resistance measurements.

Concentration of SnS in the bath ($g \cdot l^{-1}$)	Vickers hardness (load 100 g)		Weight loss (mg)	
	As plated	Annealed (250°C)	As plated	Annealed (400°C)
0	490	602	7.88	4.92
6	610	741	5.93	2.87
10	802	958	5.02	1.35
14	1004	2009	1.26	0.09
18	972	1087	4.67	3.17

Table 2 gives the results of Vickers micro hardness and wear tests obtained for Ni-P and Ni-P-SnS composite coatings both as-deposited and after heat treatment at 250°C for 4 hours. The hardness values of Ni-P coatings in the as plated and heat-treated conditions were found to be similar to those obtained in other cases for deposits with an identical phosphorous content [14, 15]. In the as plated condition, the hardness values found to increase along with the weight percentage of SnS in the plating bath increases due to the incorporation of tin sulfide particles in the Ni-P matrix.The enhanced hardness in the case of the composite (14 $g \cdot l^{-1}$ of SnS) after annealing at 250°C for 4 h is ascribed to the precipitation of intermetallic phases encouraged by SnS particles. As a result, the composite is anticipated to contain significant amounts of Ni_3P phase, which produces the relieved film. Both the hard tin sulfide particles and the Ni_3P phases present in the coatings matrix can be attributed for the increased hardness value of coatings comprising Ni – 8.87% P – 7.62% SnS. Wear resistance of Ni – 8.87% P – 7.62% SnS is higher than that of Ni – 10.84% P – 0% SnS, indicating that SnS particles in the coatings are the reason for the better outcomes. Following the heat treatment process, the coatings' wear resistances have increased. Figure 1 shows the relationship between the coefficients of friction and sliding time of Ni-P and Ni-P-SnS coatings. It was observed that both specimens' coefficients of friction are comparable at 0.1 up to a sliding duration of 90 seconds. With increasing sliding times up to 600 seconds, the Ni-P coatings' coefficient of friction rises from 0.1 to 0.189 after 90 seconds. Contrarily, the Ni-P-SnS coatings exhibit a constant coefficient of friction of 0.138 up to a sliding distance of 600 seconds, indicating that the layers of the composite were not peeled off during the tests. This technique confirmed that SnS thin films obtained by electroless deposition had improved the tribological characteristics of Al 6061 and reduced the frictional coefficient of Ni-P on aluminum substrate.

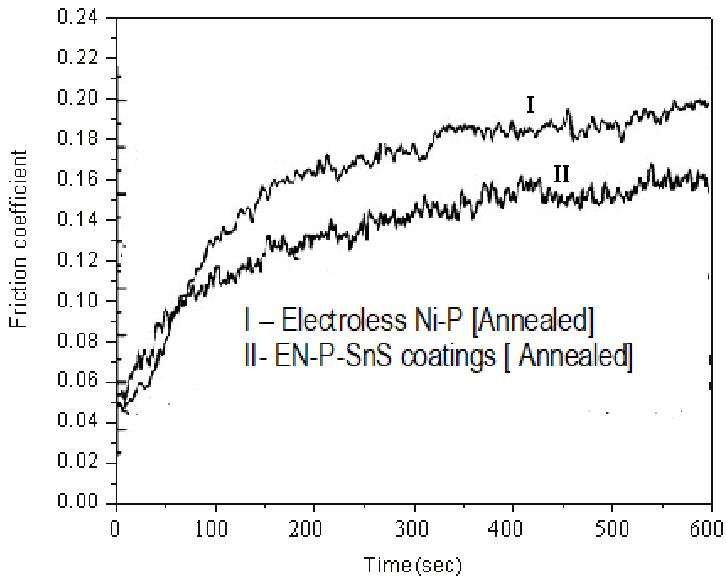

Figure 1. Frictional coefficient studies of coatings.

3.2. Corrosion resistance measurements

Nyquist diagrams for electrolessly deposited Ni-P (annealed), Ni-P-SnS and Ni-P-SnS (annealed) composite coatings measured in 3.5% NaCl solution are given in figure 2.

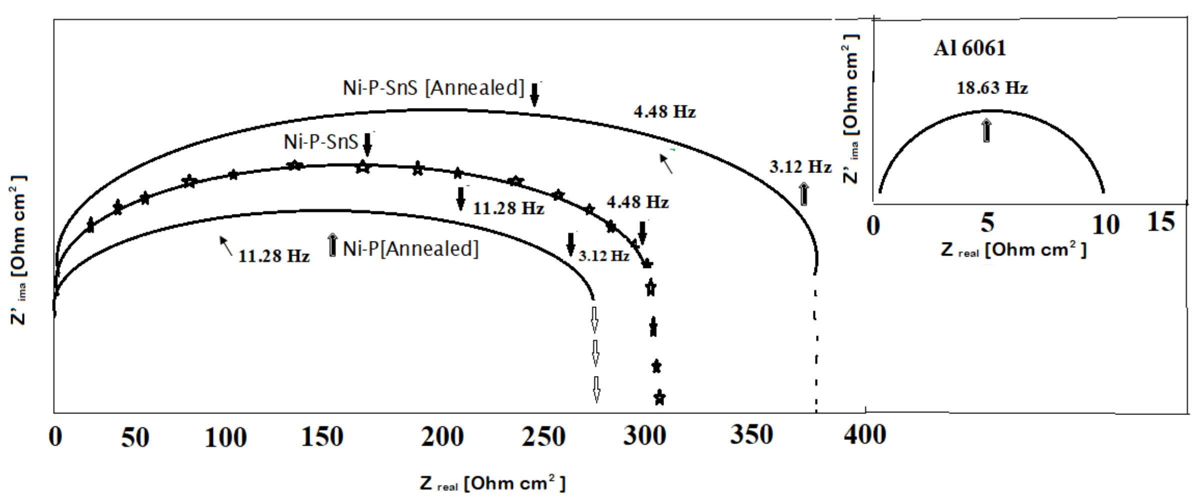

Figure 2. Corrosion resistance studies of Ni-P-SnS deposits on Al 6061 alloy using Impedance studies [Electrolyte 3.5% NaCl].

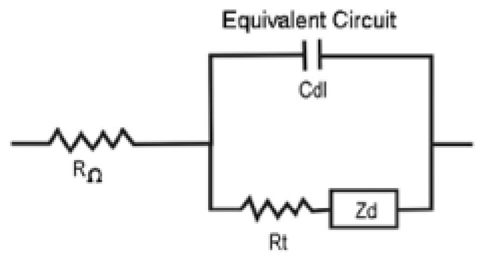

Figure 3. Equivalent circuit analysis with EIS data.

The R_t and C_{dl} values of coatings are shown in Table 3. It is well evidenced that annealed SnS incorporated electroless Ni-P coatings on Al 6061 is showing better corrosion resistance than Al 6061 alloy in 3.5% NaCl. The Nyquist plot is shown in Figure 2 in both the absence and presence of the electroless Ni-P-SnS deposits in 3.5% NaCl. According to Figure 2, the impedance characteristics of Al-6061 significantly changed in the presence of electroless deposits and the diameter of the Nyquist plot increased, indicating that the corrosion of Al-6061 is primarily a charge transfer process. A depressed capacitive loop is visible in the high frequency (HF) portion of the Nyquist plot. Surface non-homogeneity of the interfacial origin and the charge transfer process are both quoted as contributing factors to the depressed capacitive loop.

According to Figure 3, the corrosion of metals in aggressive ions media is a phenomenon controlled by charge transfer, and the interpretation of the impedance data is typically based on the usage of an equivalent circuit. The circuit's proper arrangement of basic electrical components, such as capacitors and resistors, allows it to describe the electrochemical reaction taking place at the metal electrolyte interface. Table 3 contains the various impedance characteristics, including R_{ct} or R_t, R_s, n, C_{dl}, and, that were obtained using the Nyquist plot. The as plated electroless Ni-P-SnS and electroless Ni-P-SnS after annealed condition caused a large increase in R_{ct} value, indicating that electroless deposits have completely covered on surface of Al-6061.

The local dielectric constant's decline and/or the thickness of the electric double layer's growth are both possible causes of the drop in C_{dl} value. This discovery makes yet another case for the development of an electroless Ni-P-SnS protective coating on Al-6061 surfaces. Table 3 also shows that the values of phase shift (n) are higher in the presence of electroless Ni-P-SnS deposits than in the Al-6061 without plating. The heterogeneity or roughness of the surface was connected to the value of n. The larger surface roughness is typically related with smaller values of n. The results shown in Table 3 show that the values of n are higher when electroless Ni-P deposits are present (0.833–0.895) than the absence of electroless plated surface (0.830), indicating that surface roughness is noticeably reduced when electroless Ni-P-SnS deposits are present because Ni-P-SnS electroless deposits form a soft layers on the surface of Al 6061.

Table 3. Evaluation of corrosion resistance of the coatings by impedance measurements obtained from Nyquist plots: Electrolyte 3.5% NaCl.

Materials used	R_s	R_{ct} or R_t	C_{dl}	n	θ	%
Al 6061	1.17	9.87	105.81	0.830	–	–
Electroless Ni-P on Al 6061 [annealed]	1.009	252.81	37.39	0.833	0.9609	96.09
Electroless Ni-P-S on Al 6061 [as plated]	1.079	295.67	36.07	0.872	0.9666	96.66
Electroless Ni-P-S on Al 6061 [after annealing]	1.144	375.58	21.99	0.895	0.9737	97.37

The R_t of Ni-P-SnS (annealed) with 14 $g\cdot l^{-1}$ SnS and Ni-P (annealed) composite coatings are 375.58 and 252.81 Ohm/cm^2, respectively and the resultant C_{dl} values are 21.99 and 37.39 $\mu F\cdot cm^{-2}$. Li [16] and Karthikeyan *et al*. [17] studied that the high values of R_t and low values of C_{dl} designate better corrosion protective ability of coatings, while the C_{dl} value is also associated to the porosity of the coating. The percentage of corrosion protection has been calculated by subtracting the R_t values of electroless deposited Ni-P alloys from non deposited Al 6061, the values were divided by R_t values of electroless deposited Ni-P alloys and the resultant factors were converted into percentage. The composite coatings demonstrated the best corrosion resistance properties of electroless deposits are in consistent with hardness and wear resistance results.

3.3. Influence of tin sulfide particulate concentrations in the plating formulation on the percentage of nickel and phosphorous in the deposit

According to Table 4, adding more SnS to the plating formulation improves the integration of SnS into the Ni-P matrix. The percentages of nickel and phosphorus in the deposits have decreased due to rising SnS concentrations. The recommended dosage for the bath is 14 $g\cdot l^{-1}$ of SnS, which is the optimal concentration. Beyond these, the intense particle collisions further impair plating.

The integration of SnS appears to be mechanical and minor hydrophobic particle electrophoretic effects. The particles are incorporated into the nickel alloy being deposited and become a part of the cermets as they strike the Al 6061 surface. SnS particles and the Ni-P matrix do not share any molecules [18]. The tin sulfide and Ni, P particles that encircled the tin sulfide and invaded the surface of the Al 6061 alloy during deposition then served as the matrix material to establish the composite mechanically. The homogeneity of coatings may be ensured by agitating the plating bath while rotating the Al 6061 substrate and evenly retaining SnS as suspended powders.

Table 4. Effect of concentration of SnS particles in the bath on the percentage of Ni, P and SnS particle in the deposit.

SnS in the bath ($g \cdot l^{-1}$)	Composition of the deposit		
	Nickel (%)	Phosphorus (%)	SnS (%)
0	89.16	10.84	–
6	87.60	9.83	2.57
10	84.88	9.12	6.00
14	83.51	8.87	7.62
18	86.13	7.92	5.95

3.4. XRD measurements

Diffractograms of electroless Ni-P and Ni-P-SnS composite coatings, following heat treatment, are shown in Figure 4. The nickel phosphide (Ni_3P) intermetallic phase precipitated in the matrix after 4 hours of heating to 250°C, and diffractograms display separate peaks corresponding to crystalline Ni_3P and integrated SnS particles. The heat treatment technique causes the deposit grains to expand significantly, resulting in a substantial amount of SnS crystallites.

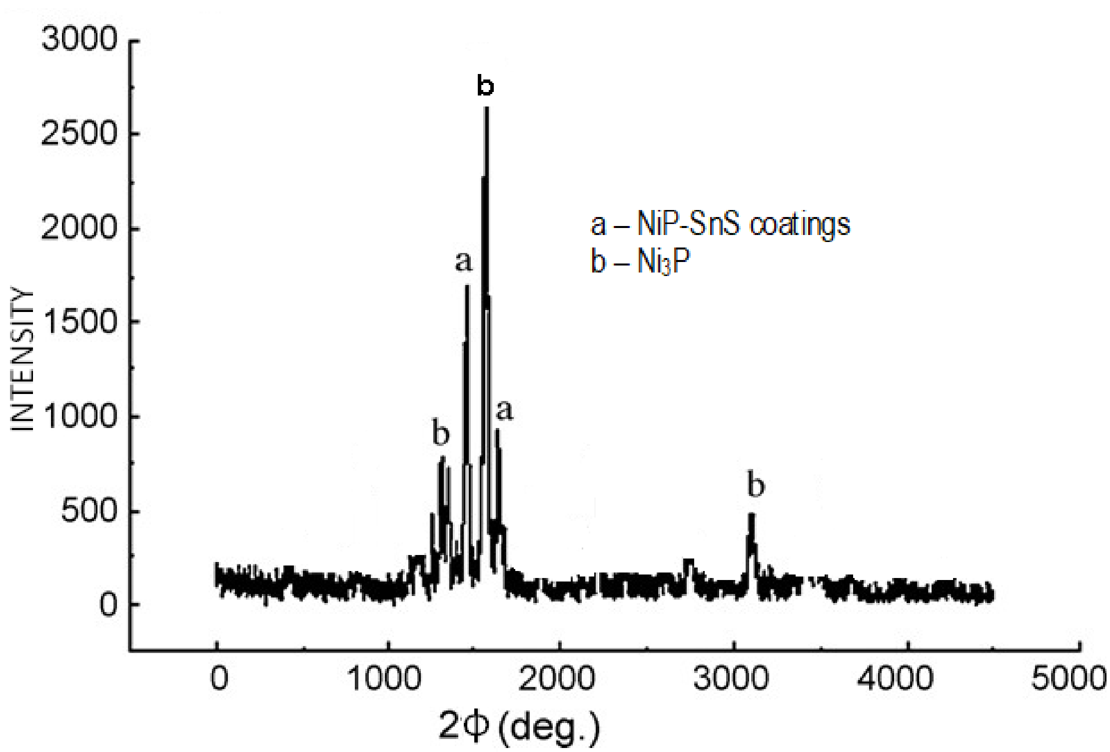

Figure 4. X-ray diffraction patterns of the annealed coatings.

4. Conclusions

Electroless plating was used to create a new Ni-P-SnS composite coating on Al 6061 alloy. X-ray diffractograms have proven that coatings containing tin sulfide particles are in their crystallized condition. Ni-P-SnS composite coatings exhibit significantly greater microhardness, wear resistance, and corrosion resistance than Ni-P coatings. Because of the coatings' low coefficient of friction, they can be used as solid lubricants on the moving parts of electronic machinery.

References

1. R. Chakrabarti, S.B. Hota and P.B. Mandal, Synthesis and Comparative Characterization of Electroless Ni-P, Ni-P-nano-Al_2O_3 and Duplex Ni-P/Ni-P-nano-Al_2O_3 Coatings on Aerospace-Graded AA2024 alloy, *Lecture Notes in Mechanical Engineering*, Springer, Singapore, 2022, pp. 73–81. doi: 10.1007/978-981-16-8724-2_7
2. M. Azadi, H. Tavakoli, S. Haghighatkhah and F.A. Eranegh, Electrochemical Characteristics of Various Ni-P Composite Coatings in 0.6 M NaCl Solution, *Trans. Indian Inst. Met*., 2021, **74**, 137–147. doi: 10.1007/s12666-020-02125-1
3. N. Jamal, S. Mohanty, S. Raj and A.K. Das, Composite Coating on Aluminum-Based Alloys through Ni-P Electroless Plating Route. *Lecture Notes in Mechanical Engineering*, Springer, Singapore, 2021, pp. 93–102. doi: 10.1007/978-981-33-6029-7_9
4. G. Oppong Boakye, A.M. Ormsdóttir, B.G. Gunnarsson, S. Irukuvarghula, R. Khan and S.N. Karlsdóttir, The Effect of Polytetrafluoroethylene (PTFE) Particles on Microstructural and Tribological Properties of Electroless Ni-P+PTFE Duplex Coatings Developed for Geothermal Applications, *Coatings*, 2021, **11**, no. 6, 670. doi: 10.3390/coatings11060670
5. Z. Liu, Z. Chen, W. Li, Z. Ding and Z. Xu, Composite Fouling Characteristics on Ni-P-PTFE Nanocomposite Surface in Corrugated Plate Heat Exchanger, *Heat Transfer Eng*., 2021, **42**, no. 22, 1877–1888. doi: 10.1080/01457632.2020.1834202
6. A. Tang, M. Wang, W. Huang and X. Wang, Composition design of Ni-nano-Al2O3-PTFE coatings and their tribological characteristics, *Surf. Coat. Technol*., 2015, **282**, 121–128. doi: 10.1016/j.surfcoat.2015.10.034
7. Z. Zhang, J. Xian, H. Wu, M. Jin and Z. Shen, Influence of particle concentration on the elemental penetration region and properties of Ni-P-SiC composite coatings prepared through sandblasting and scanning electrodeposition on 45 steel surfaces, *Coatings*, 2021, **11**, no. 10, 1237 doi: 10.3390/coatings11101237
8. M. Ram, S. Sharma, A. Ansari and A.K. Sharma, Surface modification of mild steel by electroless Ni-P-SiC nanocomposite coating and its corrosion and tribological resistance, *AIP Conference Proceedings 2335*, 2021, 080010. doi: 10.1063/5.0043715
9. P. Chandrasekar and D. Nagaraju, Improvement of Bonding Strength at the Interfaces in Scrap Al Alloy Composites Using Electroless Ni-P Coated SiC, *Silicon*, 2022, **14**, 2941–2952. doi: 10.1007/s12633-021-01078-4

10. V.B. Chintada, R. Koona and M.V.A. Raju Bahubalendruni, State of Art Review on Nickel-Based Electroless Coatings and Materials, *J. Bio Tribo Corros.*, 2021, **7**, 134. doi: 10.1007/s40735-021-00568-7
11. K. Czapczyk, P. Zawadzki, N. Wierzbicka and R. Talar, Microstructure and Properties Of Electroless Ni-P/Si_3N_4 Nanocomposite Coatings Deposited On The AW-7075 Aluminum Alloy, *Materials*, 2021, **14**, no. 16, 4487. doi: 10.3390/ma14164487
12. M. Badihehaghdam, S.M. Mousavi Khoie, F. Khast and M. Safarzadeh Khosrowshahi, Mechanical Properties and Electrochemical Behavior of Electroless Ni-P-AlN Nanocomposite Coating, *Met. Mater. Int.*, 2022, **28**, 1372–1385. doi: 10.1007/s12540-021-00994-9
13. P.-C. Huang, K.-H. Hou, J.-J. Hong, M.-H. Lin and G.-L. Wang, Study of fabrication and wear properties of Ni-SiC composite coatings on A356 aluminum alloy, *Wear*, 2021, **477**, 203772. doi: 10.1016/j.wear.2021.203772
14. G.P. Ram, S. Karthikeyan, P.E. Nicholas and A.S. Sofia, Dry sliding wear behavior of electroless NIP and NIP-Al_2O_3 composite coatings, *Mater. Today: Proc.*, 2021, **37**, 2001–2009. doi: 10.1016/j.matpr.2020.07.495
15. S. Roy, B.M. Mishra and G.K. Bos, Characterization of Ni-P based poly-alloy and composite coatings involving nanoindentation and nanoscratch tests, *Mater. Today Commun.*, 2021, **29**, 102991. doi: 10.1016/j.mtcomm.2021.102991
16. A.P. Meshram, A. Gupta and C. Srivastava, Effect of electrodeposition temperature on texture, strain, grain boundary constitution and corrosion behavior of Ni-P coatings with low phosphorous content, *Materialia*, 2022, **22**, 101413. doi: 10.1016/j.mtla.2022.101413
17. K.S. Abdel Halim, M. Ramadan, E.-S.M. Sherif, K.M. Hafez, T. Subhani, N. Fathy, A.S. Alghamdi and M.H. Khedr, Enhancement of Surface and Interface Properties of Low Carbon Steel by Hybrid ZnO and NiO Nanoparticles Reinforced Tin Coating, *Crystals*, 2022, **12**, no. 3, 332. doi: 10.3390/cryst12030332
18. M. Czagány and P. Baumli, Effect of tin addition on the properties of electroless Ni-P coatings, *Mater. Sci. Eng.*, 2020, **45**, no. 1, 50–62. doi: 10.32974.mse.2020.005

♦ ♦ ♦